Available online at www.sciencedirect.com
SCIENCE DIRECT®
International Journal of Heat and Mass Transfer 48 (2005) 3493–3505
International Journal of HEAT and MASS TRANSFER
www.elsevier.com/locate/ijhmt

Natural convection in cavities with a thin fin on the hot wall

E. Bilgen *

Ecole Polytechnique Box 6079, Centre Ville, Montreal, QC, Canada H3C 3A7

Received 25 September 2004; received in revised form 25 March 2005
Available online 23 May 2005

Abstract

A numerical study has been carried out in differentially heated square cavities, which are formed by horizontal adiabatic walls and vertical isothermal walls. A thin fin is attached on the active wall. Heat transfer by natural convection is studied by numerically solving equations of mass, momentum and energy. Streamlines and isotherms are produced, heat and mass transfer is calculated. A parametric study is carried out using following parameters: Rayleigh number from 10^4 to 10^9, dimensionless thin fin length from 0.10 to 0.90, dimensionless thin fin position from 0 to 0.90, dimensionless conductivity ratio of thin fin from 0 (perfectly insulating) to 60. It is found that Nusselt number is an increasing function of Rayleigh number, and a decreasing function of fin length and relative conductivity ratio. There is always an optimum fin position, which is often at the center or near center of the cavity, which makes heat transfer by natural convection minimized. The heat transfer may be suppressed up to 38% by choosing appropriate thermal and geometrical fin parameters.

1. Introduction

Natural convection heat transfer in differentially heated, partitioned cavities are encountered in various industrial applications, such as heating and ventilating of living spaces, fire in buildings, solar thermal collector systems, electronic cooling devices, in storage of radioactive wastes. Studies of various aspects of this problem have been carried out by many researchers both theoretically and experimentally.

Excluding studies with multiple fins in tall systems (see, for example, [1–3]), thick fin(s) in square and tall cavities (see, for example, [4–6]), the specific problem studied in this work involving a single thin fin attached to the hot or cold wall makes a distinct category, which has been studied by various researchers that we will briefly review [7–11]. Oosthuizen and Paul [7] studied differentially heated cavities with aspect ratio between 3 and 7 with a horizontal plate attached to the center of the cold vertical wall. They found the local heat transfer rate on the upper portion of the hot wall increased, but the heat transfer rate near the center of the hot wall decreased. Frederick [8] studied a similar situation in a inclined cavity with diathermal partition at Rayleigh number between 10^3 and 10^5. The partition was attached to the cold wall at its center, its relative length was 0.25 and 0.50. The inclination angle was from 90° (corresponding to horizontal partition) to 45°. His results showed that the partition caused suppression of convection and the heat transfer relative to that in an identical cavity without partition was reduced considerably. Frederick and Valencia [9] studied natural convection in a square cavity with a conducting partition at the center of its hot wall and with perfectly conducting

* Tel.: +1 514 340 4711x4579; fax: +1 514 340 5917.
E-mail address: bilgen@polymtl.ca

0017-9310/$ - see front matter © 2005 Elsevier Ltd. All rights reserved.
doi:10.1016/j.ijheatmasstransfer.2005.03.016

Nomenclature

A	cavity aspect ratio, H/L
Y_P	dimensionless thin fin position, h/H
W_P	dimensionless thin fin length, w/H
c_p	heat capacity, J/kg K
g	acceleration due to gravity, m/s^2
H	cavity height, m
k	thermal conductivity, W/m K
k_r	dimensionless conductivity, k_{fin}/k_a
L	cavity width, m
Nu	Nusselt number, Eq. (5)
p	pressure, Pa
P	dimensionless pressure, $(p-p_\infty)L^2/\rho\alpha^2$
Pr	Prandtl number, v/α
Ra	Rayleigh number, $g\beta\Delta TL^3/(v\alpha k)$
t	time, s
T	temperature, K
U, V	dimensionless fluid velocities, uL/α,vL/α
X, Y	dimensionless Cartesian coordinates, = x/L, y/L
x, y	Cartesian coordinates

Greek symbols

α	thermal diffusivity, m^2/s
β	volumetric coefficient of thermal expansion, 1/K
v	kinematic viscosity, m^2/s
ρ	fluid density, kg/m^3
ψ	stream function
θ	dimensionless temperature, $(T-T_C)/(T_H-T_C)$
τ	dimensionless time, $\alpha t/L^2$

Subscripts

a	air
C	cold, ambient value
ext	extremum
f	fluid
fin	fin
H	hot, active
loc	local
max	maximum
min	minimum

Superscript

–	average

horizontal walls. Partition length and its conductivity were variable. For low values of relative conductivity, they reported reduced heat transfer with respect to that in an identical cavity without partition at Rayleigh numbers between 10^4 and 10^5. Nag et al. [10] studied numerically in a differentially heated square cavity where a horizontal plate was attached on the hot wall. The length and the position of the partition were varied and Rayleigh was between 10^3 and 10^6. They considered two cases, one with adiabatic partition and the other with perfectly conducting partition. They found that with the perfectly conducting partition the heat transfer at the cold wall increased irrespective of its position or length and it is attenuated with the adiabatic partition, which was more pronounced when the position of the partition was higher. Shi and Khodadadi [11] studied numerically the same problem reported by Nag et al. with almost perfectly conducting partition on the hot wall, but with more extensive parametric details. Their dimensionless fin length was between 0.20 and 0.50, which had seven positions along the hot wall and Rayleigh number was from 10^4 to 10^7. Since the fin was almost perfectly conducting and attached to the hot wall, the fin's heating enhanced the convection while its blockage of the flow field suppressed it. The contribution of these two counter-acting mechanisms were not clearly quantified. Based on the numerical data, they proposed correlations to calculate Nusselt number as a function of relevant parameters for this particular case.

We see from this brief review that excluding that by Frederick and Valencia [9], all other studies considered only the perfectly conducting or insulated partitions. Yet, in practical engineering problems, often partitions are made from materials with finite conductivities. In this paper, we will study the case with dimensionless fin length from 0.10 to 0.90 at dimensionless fin position from 0.10 to 0.90 and fin to air conductivity ratio from 0 (perfectly insulating materials) to 60 (construction and fabrication materials) and examine heat transfer by conduction and convection due to fins with finite conductivity ratios.

2. Problem and mathematical model

2.1. Problem definition

A schematic of the two dimensional system is shown in Fig. 1. The square cavity is differentially heated, the left isothermal wall is at T_H and the right at T_C with horizontal walls insulated. A thin fin of W_P long is attached

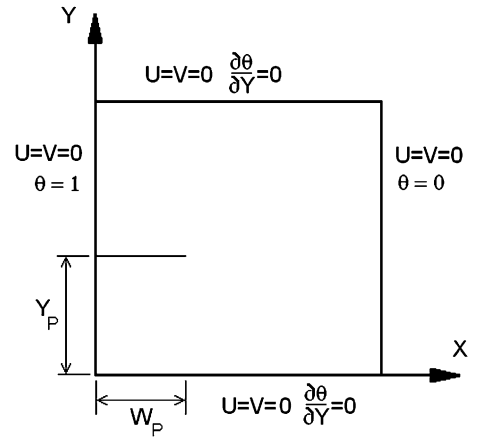

Fig. 1. Schematic of the square cavity with thin fin attached on the hot wall, the coordinate system and boundary conditions.

to the active wall at a height Y_P. The coordinate system and boundary conditions are also shown in Fig. 1.

2.2. Mathematical model

The continuity, momentum and energy equations for a two dimensional laminar flow of an incompressible Newtonian fluid are written. Following assumptions are made: there is no viscous dissipation, the gravity acts in the vertical direction, fluid properties are constant and fluid density variations are neglected except in the buoyancy term (the Boussinesq approximation) and radiation heat exchange is negligible. Using non-dimensional variables defined in the nomenclature, the non-dimensional governing equations are obtained as

$$\frac{\partial U}{\partial X}+\frac{\partial V}{\partial Y}=0 \tag{1}$$

$$\frac{\partial U}{\partial \tau}+U\frac{\partial U}{\partial X}+V\frac{\partial U}{\partial Y}=-\frac{\partial P}{\partial X}+Pr\nabla^2 U \tag{2}$$

$$\frac{\partial V}{\partial \tau}+U\frac{\partial V}{\partial X}+V\frac{\partial V}{\partial Y}=-\frac{\partial P}{\partial Y}+Pr\nabla^2 V+Ra\,Pr\theta \tag{3}$$

$$\frac{\partial \theta}{\partial \tau}+U\frac{\partial \theta}{\partial X}+V\frac{\partial \theta}{\partial Y}=\nabla^2\theta \tag{4}$$

The steady-state solutions are obtained from unsteady-state equations, Eqs. (1)–(4). The local, average and normalized average Nusselt numbers are calculated respectively as

$$\left.\begin{aligned} Nu_{\mathrm{loc}} &= -\frac{\frac{\partial\theta}{\partial X}}{\theta}\\ \overline{Nu} &= \int_0^A Nu_{\mathrm{loc}}\,\mathrm{d}Y\\ Nu &= \frac{\overline{Nu}_{Ra}}{\overline{Nu}_{Ra=0}} \end{aligned}\right\} \tag{5}$$

The stream function is calculated from its definition as

$$U=-\frac{\partial\psi}{\partial Y},\quad V=\frac{\partial\psi}{\partial X} \tag{6}$$

where ψ is zero on the solid surfaces and the streamlines are drawn by $\Delta\psi=(\psi_{\max}-\psi_{\min})/n$ with n = number of increments.

2.3. Boundary conditions

The boundary conditions of the system shown in Fig. 1 are $U=V=0$ on all solid surfaces, $\frac{\partial P}{\partial n}=0$ on all solid surfaces at the outside boundaries. On the adiabatic boundaries, $\frac{\partial\theta}{\partial n}=0$. Thus,

$$\left.\begin{aligned} &\text{On all solid boundaries}: \quad U=V=0\\ &\text{at } X=0 \quad \frac{\partial P}{\partial X}=0,\quad \theta=1\\ &\text{at } X=1 \quad \frac{\partial P}{\partial X}=0,\quad \theta=0\\ &\text{at } Y=0 \text{ and } Y=1 \quad \frac{\partial P}{\partial Y}=0,\quad \frac{\partial\theta}{\partial Y}=0 \end{aligned}\right\} \tag{7}$$

3. Numerical technique

The numerical method used to solve Eqs. (1)–(4) is the SIMPLER (semi-implicit method for pressure linked equations revised) algorithm [12]. The computer code based on the mathematical formulation discussed earlier and the SIMPLER method were validated for various cases published in the literature, the results of which are discussed elsewhere [13].

Non-uniform grid in X and Y direction were used for all computations. Grid convergence was studied for the case of $W_P=0.5$ with grid sizes from 20×20 to 80×80 at $Ra=10^5$. Grid independence was achieved within 1.2% in Nusselt number with grid size of 40×40. Similar tests were done with the cavities having thin fin at different positions with different length, and found that the grid size was satisfactory. For the thin fin, four mesh points were used and its dimensionless thickness was 0.01. Using a system with 2.0 GHz clock speed, a typical execution time (real time), at $Ra=10^5$ for example, was 31.65 s and the number of iteration was 3260.

The accuracy control was carried out by the conservation of mass by setting its variation to less than 10^{-3}, on the pressure term by setting the variation of residues at 10^{-3}. In addition, the accuracy of computations was checked using the energy conservation within the system, by setting its variation to less than 10^{-4}.

The natural convection in the undivided square cavity is calculated for Ra from 10^4 to 10^9 and shown in Table 1, where the results with the mesh size of 40×40 of the benchmark case is also given for 10^5

Table 1
Validation in a square cavity

Ra	*Nu* [14]	*Nu* (this study)	$\lvert\Psi_{ext}\rvert$ [14]	$\lvert\Psi_{ext}\rvert$(this study)
10^4	2.246	2.245	–	5.07536 (0.5, 0.5)
10^5	4.511	4.521	9.601 (0.2875, 0.6)	9.599 (0.2962, 0.585)
10^6	8.777	8.800	16.954 (0.15, 0.55)	17.035 (0.1649, 0.5424)
10^7		16.6287		31.113 (0.0940, 0.5424)
10^8		31.5202		56.9806 (0.0462, 0.5424)
10^9		60.7284		103.3060 (0.0244, 0.5424)

and 10^6 [14]. It is seen that the agreement is very good: The deviation in Nusselt number obtained by the code is 0.22% for $Ra = 10^5$ and 0.26% for $Ra = 10^6$, while that in $|\Psi_{ext}|$ is 0.02% and 0.48% respectively. As a further check, the average Nusselt numbers at the hot and cold walls were compared, which showed a maximum difference of about 0.5% in all runs.

4. Results and discussion

Geometrical and thermal parameters governing the heat transfer in differentially heated square cavities with thin fin attached to the active wall are: aspect ratio $A = L/H = 1$, the length of thin fin, $W_P = 0$, 0.1, 0.3, 0.5, 0.7, 0.9, the position of thin fin, $Y_P = 0$, 0.10, 0.30, 0.50, 0.70, 0.90, the dimensionless conductivity of thin fin, $k_r = 0$, 1, 30, 60. Thus, the cases considered were 144 all together. Rayleigh number was varied from 10^4 to 10^9.

Flow and temperature fields, and heat transfer through the cavity are examined. All results are with $Pr = 0.7$. First, we will present flow and temperature fields for typical cases, then we will present the normalized *Nu* number calculated by Eq. (5) as a function of Rayleigh number and the other non-dimensional parameters.

4.1. Flow and temperature fields

Flow and temperature fields for the square cavity without fin and for $Ra = 10^4$, 10^6 and 10^8 are presented in Fig. 2 as reference. *Nu* and $|\Psi_{ext}|$ for various Rayleigh numbers are given in Table 1.

Flow and temperature fields for typical cases are presented for $Ra = 10^6$ in Fig. 3. The conductivity ratio is constant, $r_k = 30$, the dimensionless fin length, W_P is 0.3 (the first column), 0.5 (the middle column) and 0.7 (the last column) and the dimensionless fin position Y_P is from 0.1 (the first raw) to 0.9 (the last row) with 0.2 increment. The flow fields are presented in Fig. 3(a). The columns show the effect of fin position, Y_P while the rows the effect of fin length, W_P on the flow fields. The reference value for the square cavity without fin from Table 1 is: for $Ra = 10^6$, $|\Psi_{ext}| = 17.035$ at ($X = 0.1649$, $Y = 0.5424$). We note that the appearance of the flow fields in all cases is similar to the case of square cavity without fin for $Ra = 10^6$ in Fig. 2, but with certain modifications due to fins.

The first column is with constant fin length $W_P = 0.3$. When the fin is positioned at $Y_P = 0.1$, the circulation is above the fin with $|\Psi_{ext}| = 16.32$ located near the hot wall at ($X = 0.15$, $Y = 0.58$). For the fin at $Y_P = 0.3$, a small circulation develops below the fin and $|\Psi_{ext}|$, reduced slightly to 16.12, is moved to ($X = 0.85$, $Y = 0.48$) near the cold wall. This is due to the constriction encountered at the hot wall. For the fin positioned at the center, $Y_P = 0.5$, the circulation below the fin is relatively stronger and more complete, as a result of which the flow around the fin is with a vortex formed on the fin. $|\Psi_{ext}|$ is increased to 18.55 and located near the center of the cavity at ($X = 0.49$, $Y = 0.59$). When the fin position becomes higher, similar to observations regarding the first two cases, for $Y_P = 0.7$, a formation of a weak circulation above the fin is observed while for $Y_P = 0.9$, there is no visible flow above the fin. In these cases, $|\Psi_{ext}|$ are 18.99 at ($X = 0.49$, $Y = 0.60$) and 17.87 at ($X = 0.19$, $Y = 0.65$). Due to blocking effect of the fin, the convective flow is increased for $Y_P = 0.7$ while it decreased relatively to near $|\Psi_{ext}| = 17.035$ of the cavity without fin for $Y_P = 0.9$. We expect the combined heat transfer by conduction and convection to follow the trend observed with $|\Psi_{ext}|$.

The second column is for $W_P = 0.5$, all other parameters being the same. We can see that the flow fields are very similar to the case with $W_P = 0.3$ in the first column. $|\Psi_{ext}|$ is 16.31 at ($X = 0.17$, $Y = 0.55$) for $Y_P = 0.1$, 15.02 at ($X = 0.83$, $Y = 0.29$) for $Y_P = 0.3$, 18.43 at ($X = 0.67$, $Y = 0.94$) for $Y_P = 0.5$, 19.32 at ($X = 0.67$, $Y = 0.56$) for $Y_P = 0.7$, and 17.82 at ($X = 0.17$, $Y = 0.65$) for $Y_P = 0.9$. We note that $|\Psi_{ext}|$ and its location are changed similarly with position Y_P and in general, $|\Psi_{ext}|$ is slightly decreased due to longer fin length except for $Y_P = 0.7$, for which it is increased. The latter is due to constriction caused by the longer fin, which makes the circulation more rigorous in the lower part of the cavity.

In the third column of Fig. 3(a), the flow fields for $W_P = 0.7$ are presented with all other parameters being the same. The longer fin acts like a divider in this case and modifies the flow field with respect to the cases with

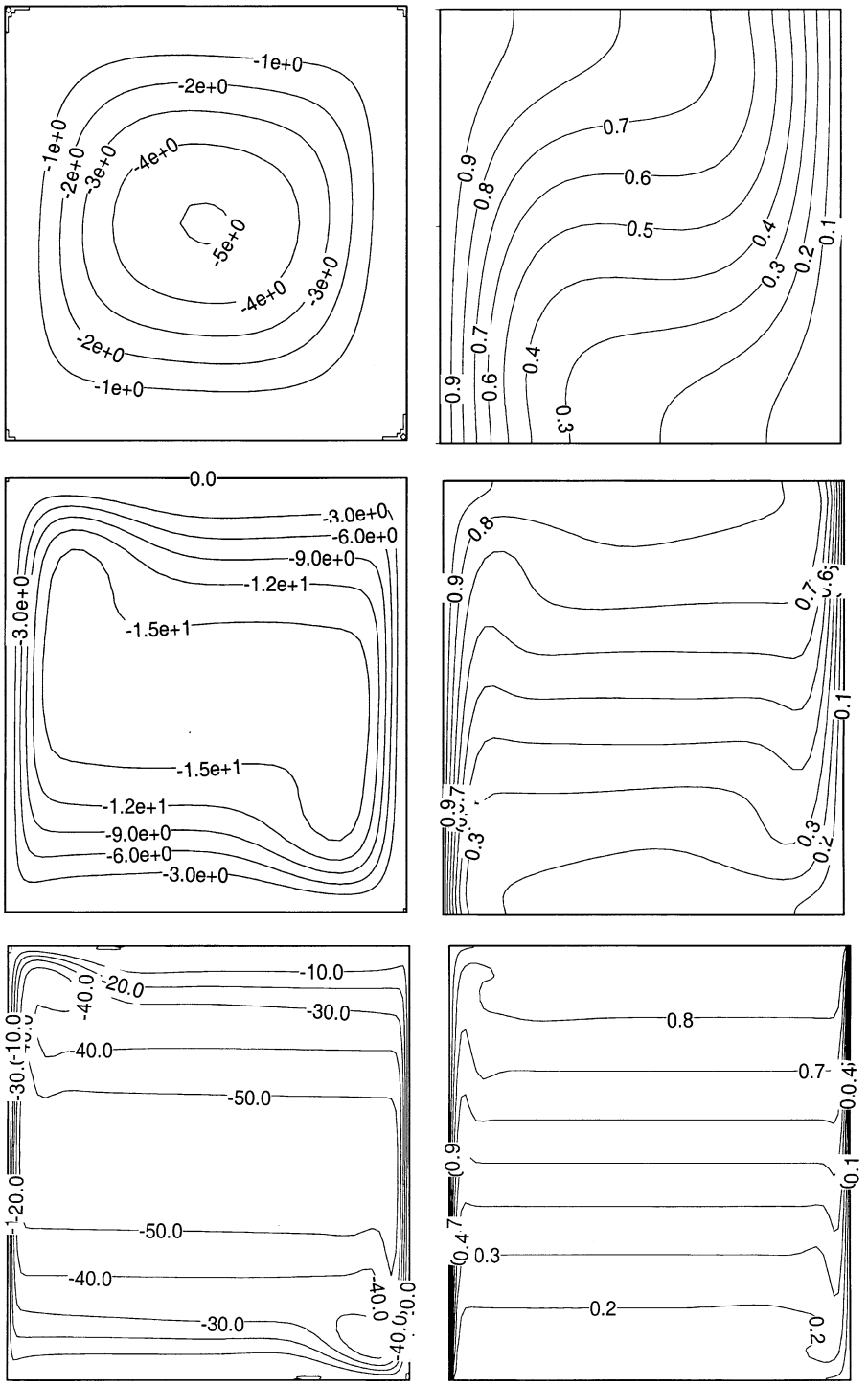

Fig. 2. Flow and temperature fields of differentially heated square cavity without fin. The first row: $Ra = 10^4$, the second row: $Ra = 10^6$ and the third row: $Ra = 10^8$. Flow field is on the left and the temperature field on the right.

shorter fins. We can see the striking similarity of the flow fields when compared to the case with $W_P = 0.5$, although the strength of $|\Psi_{ext}|$ and its location are quite different. $|\Psi_{ext}|$ is 16.42 at $(X = 0.15, Y = 0.58)$ for

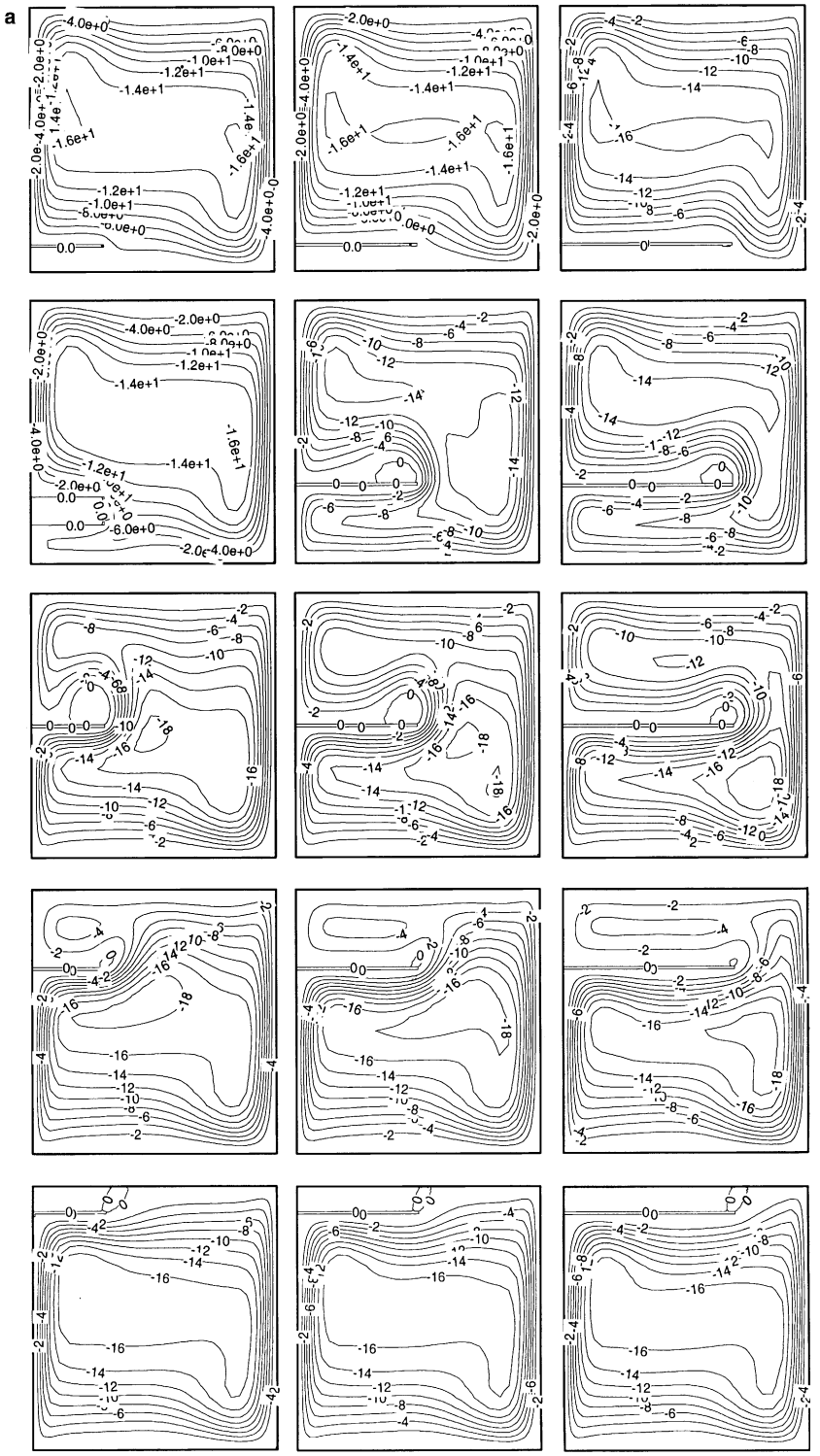

Fig. 3. (a) Flow and (b) temperature fields for $Ra = 10^6$: the first column: $W_P = 0.3$, the second column: $W_P = 0.5$, the third column: $W_P = 0.7$. The first row: $Y_P = 0.1$, the second row: $Y_P = 0.3$, the third row: $Y_P = 0.5$, the fourth row: $Y_P = 0.7$ and the fifth row: $Y_P = 0.9$.

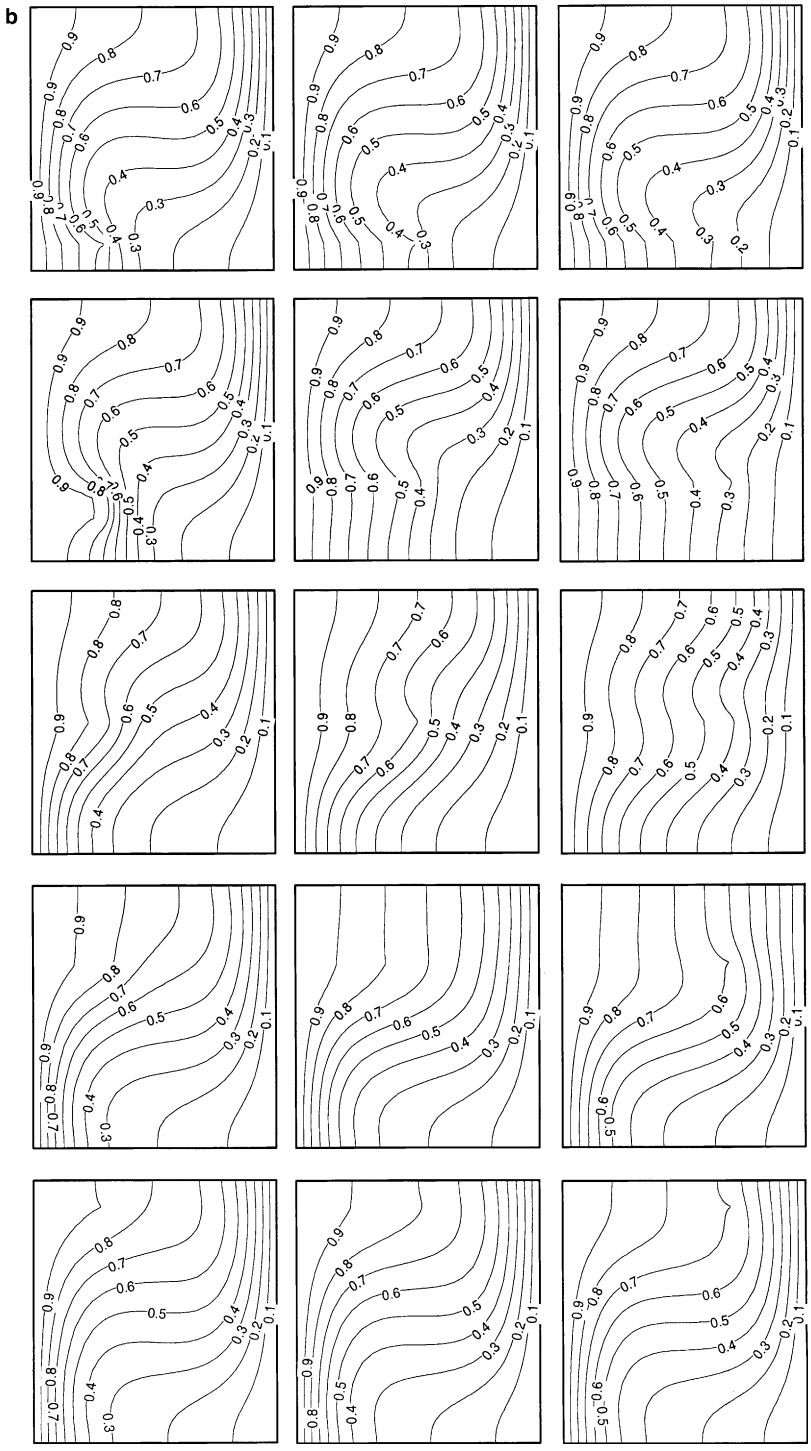

Fig. 3 (*continued*)

$Y_P = 0.1$, 15.52 at ($X = 0.47$, $Y = 0.62$) for $Y_P = 0.3$, 19.68 at ($X = 0.80$, $Y = 0.25$) for $Y_P = 0.5$, 18.80 at ($X = 0.85$, $Y = 0.41$) for $Y_P = 0.7$, and 17.46 at ($X = 0.85$, $Y = 0.45$) for $Y_P = 0.9$.

The temperature fields for the same cases as in Fig. 3(a) are arranged and presented similarly and shown in Fig. 3(b). Generally, the temperature fields in all cases are modified and instead of isotherms of a stratified fluid, there seems to be isotherms representing a conduction dominated flow field. Indeed in comparison to the square cavity without fin in Fig. 2, it appears as if the temperature fields in Fig. 3(b) correspond to $Ra = 10^4$ rather than 10^6. In the locations where the fin is attached to the hot wall, the isotherms become almost parallel to the hot wall, resulting in a modified temperature field, which influences the entire field thereafter. For the fin position of $Y_P = 0.1$, the isotherms show almost the same pattern as for $Ra = 10^4$ in a square cavity without fin in Fig. 2. As the fin position is made higher and the fin length longer, like in the case of $Y_P = 0.3$, 0.5 and $W_P = 0.7$, the isotherms become similar to a conduction dominated temperature field. There is an apparent similarity of the temperature fields between the first row and the last as well as the second row and the one before the last, i.e. the temperature fields are modified similarly for fin position with respect to the center of the cavity. The most conduction dominated like temperature field is for $Y_P = 0.5$. Although the convection suppression by the fin is an expected consequence, the observed patterns are remarkable at this high Rayleigh number.

Flow and temperature fields for $Ra = 10^4$ and 10^5 arranged similarly showed that the convection in the cavity with fin was quasi-conduction dominated as we saw in Fig. 3. Those for $Ra \geqslant 10^7$ showed stratified flow, the strength of which was increasing with Rayleigh number for the same geometrical and thermal parameters.

4.2. Heat transfer

We will present the heat transfer results in terms of normalized average Nusselt number defined by Eq. (5). The definition of the average normalized Nusselt number is based on the total heat transfer by convection and conduction of the fluid and fin divided by the conduction heat transfer of the fluid and fin. They are computed as shown in Eq. (5). Since the conductivity of fins is variable, by defining a dimensionless conductivity, $k_r = k_{fin}/k_a$, the relative fin conductivity can be used as a parameter to compare different cases with different conductivities. For example, for $k_r = 1$, we get $Nu = 1$, as we should, since the conduction heat transfer in the cavity should be the same regardless of the media filling it. For $k_r > 1$, the heat transfer by conduction should increase because of the presence of a fin with higher conductivity than air in the cavity. Indeed, this is the case: for example, with $W_P = Y_P = 0.5$, we found $Nu_{Ra=0} = 0.9948$ for $k_r = 0$, 1.0000 for $k_r = 1$, 1.1044 for $k_r = 30$ and 1.1686 for $k_r = 60$. It is clear that by using this definition, it becomes convenient to differentiate the effect of the relative conductivity. Hence, Nu is the average normalized Nusselt number and the results with square cavity without fin is included as a reference case in the following presentation of the results.

We present typical results as Nu versus Ra for the case of dimensionless fin length, $W_P = 0.3$, fin position, Y_P and conductivity ratio, k_r as parameters in Fig. 4(a)–(c). Fig. 4(a) shows the case with $k_r = 0$, the insulated fin. As we have seen before, the heat transfer by conduction in this case is slightly lower than that in a square cavity without fin and the variation in Nu represents the effect of the presence of the fin. In general, as expected the heat transfer is lowered by the fin positioned at various dimensionless height. For $Y_P = 0.5$, Nu is decreased by 27% at $Ra = 10^4$ and is 14% at $Ra = 10^9$, with 6% between 10^7 and 10^8. The change in Nu is fin position dependent: at low Rayleigh numbers, as the fin position is near center, the decrease in Nu is maximum, the reason for which follows the observations made in Fig. 3 regarding $|\Psi_{ext}|$. Fig. 4(b) shows the case with $k_r = 1$. It appears that similarly, Nu is fin position dependent, although in this case, maximum decrease of 17% is observed for $Y_P = 0.3$ at low Rayleigh numbers and Nu for $Y_P = 0.9$ is higher than that of square cavity without fin, i.e., the heat transfer is enhanced. Similar observations are made in Fig. 4(c) and (d) for $k_r = 30$ and 60: The heat transfer decrease is fin position dependent and the maximum decrease is when the fin is attached at the center, which is 21% and 18% for $k_r = 30$ and 60 respectively. These results are in accordance with the observations made in Fig. 3. We note that $Nu_{Ra=0}$ varies with fin position, passing from a maximum for $Y_P = 0.5$. For example, for $W_P = Y_P = 0.5$, $k_r = 60$, $Nu_{Ra=0} = 1.14952$ for $Y_P = 0.1$, 1.16506 for $Y_P = 0.3$, 1.16858 for $Y_P = 0.5$, 1.16538 for $Y_P = 0.7$ and 1.14995 for $Y_P = 0.9$. This shows that the heat transfer by conduction plays an important role to increase the heat transfer across the cavity, although the convection heat transfer is suppressed considerably due to presence of fins. Conversely, since the normalized Nusselt number is calculated dividing computed Nusselt number by these values, the normalized Nusselt number becomes smaller with higher $Nu_{Ra=0}$ values, the effect of which varies with Y_P.

To see the effect of the dimensionless fin length, W_P on the convection heat transfer, we present the case with fin position at $Y_P = 0.3$ for $k_r = 1$ and 60 in Fig. 5(a) and (b). As expected, in both cases Nu is a decreasing function of dimensionless fin length. For the case of $k_r = 1$, Nu is suppressed by 30% to 7% between $Ra = 10^4$ and 10^9. For the case of $k_r = 60$ in Fig. 5(b), Nu is suppressed even more by 38% to 26% between $Ra = 10^4$ and 10^9.

Fig. 6 shows the effect of the relative conductivity, k_r on the flow fields for the case of Fig. 5 for $Ra = 10^4$ and 10^8. The first row is for $k_r = 1$, the second for 30 and the third is for 60. For $Ra = 10^4$, the appearance of the flow is slightly modified when k_r is increased from 1 to 30 and

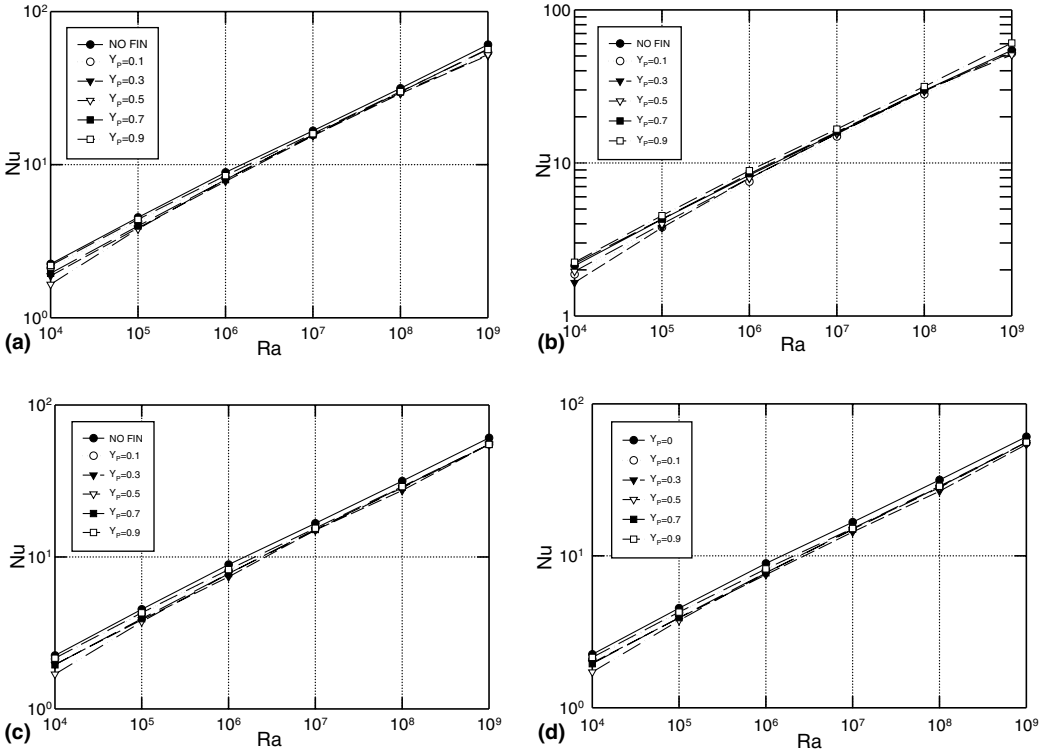

Fig. 4. Nusselt number as a function of Rayleigh number with $W_P = 0.3$ and Y_P from 0.1 to 0.9 as a parameter: (a) $k_r = 0$, (b) $k_r = 1$, (c) $k_r = 30$ and (d) $k_r = 60$.

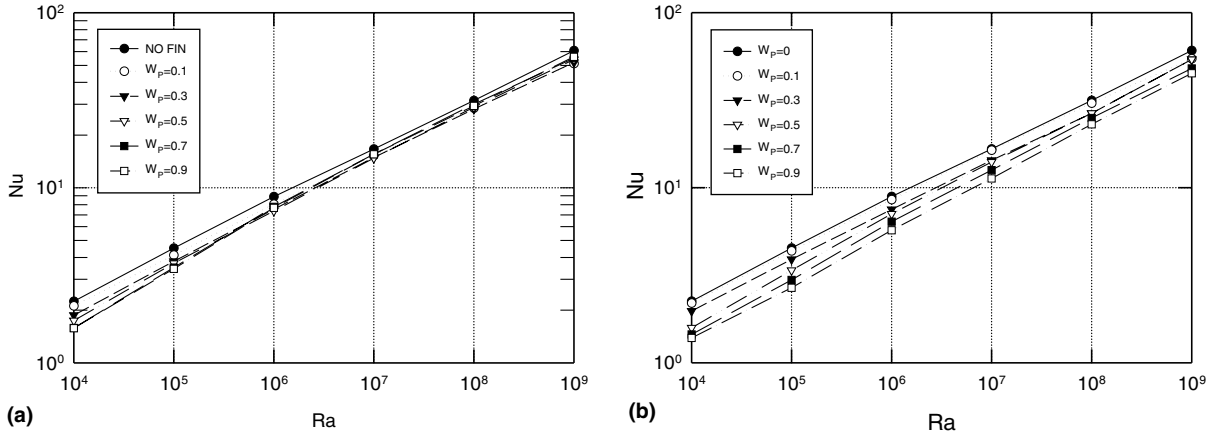

Fig. 5. Nusselt number as a function of Rayleigh number with $Y_P = 0.3$ and W_P from 0.1 to 0.9 as a parameter: (a) $k_r = 1$, (b) $k_r = 60$.

then to 60. $|\Psi_{ext}|$ is 3.62 ($X = 0.65$, $Y = 0.48$) for $k_r = 1$, 3.78 ($X = 0.65$, $Y = 0.49$) for $k_r = 30$ and 3.86 ($X = 0.65$, $Y = 0.49$) for $k_r = 60$. It is seen that the strength of circulation is enhanced by 4.4% by increasing k_r from 1 to 30 and 6.6% from 1 to 60, and the location of $|\Psi_{ext}|$ practically did not change. It is noted that $|\Psi_{ext}|$ in these three cases is lowered considerably with respect to the case of the cavity without fin, since the flow field is quasi-conductive. For $Ra = 10^8$ shown in the second column, $|\Psi_{ext}|$ is 70.32 ($X = 0.42$, $Y = 0.51$) for $k_r = 1$, 69.63 ($X = 0.40$, $Y = 0.49$) for $k_r = 30$ and 69.38 ($X = 0.40$, $Y = 0.49$) for $k_r = 60$. It is observed that due to high Rayleigh number convection, the circulation strength is decreased by 0.9% from $k_r = 1$ to 30 and 1.3% from

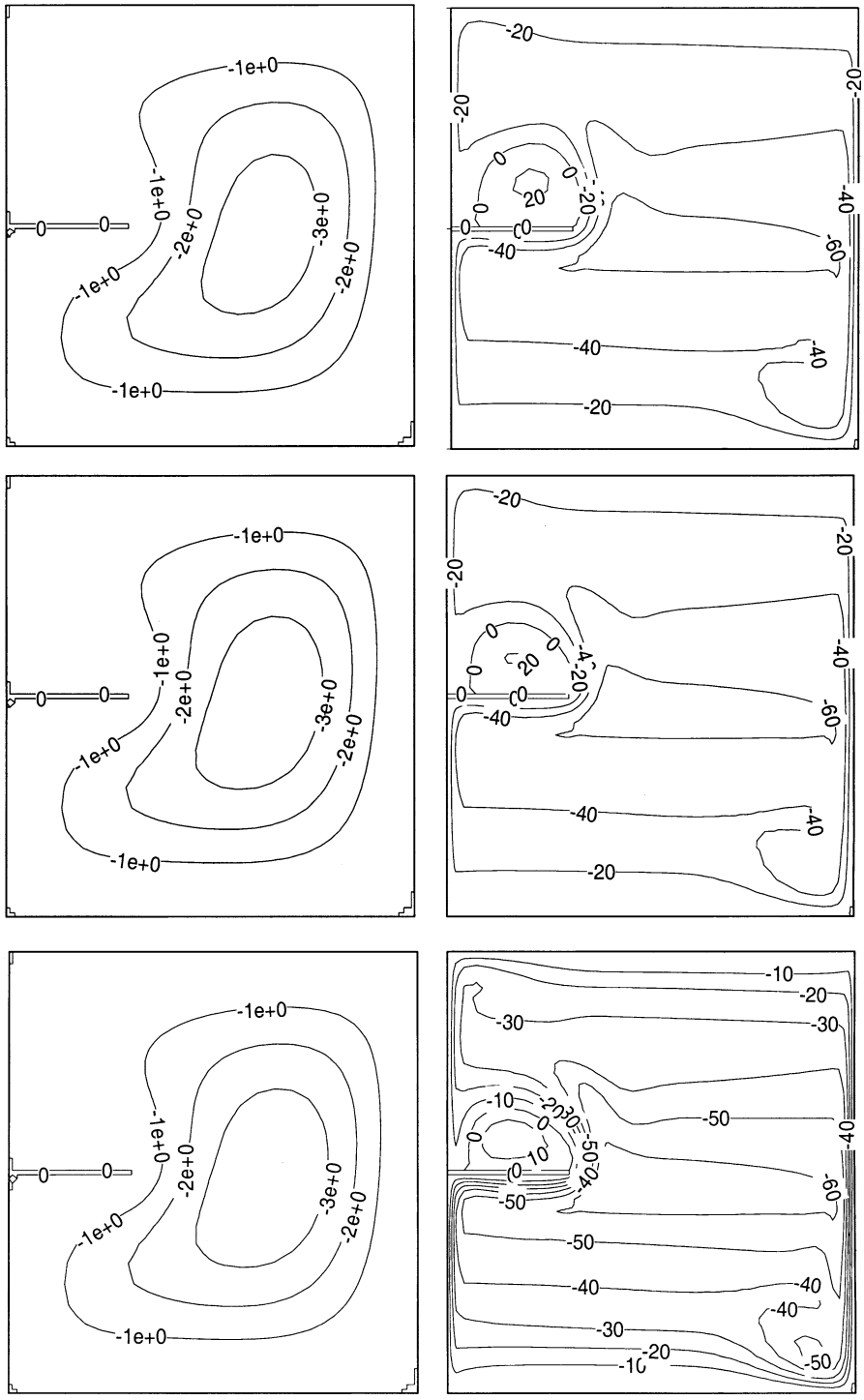

Fig. 6. Flow fields for $Ra = 10^4$ and 10^8 with $W_P = 0.3$ and $Y_P = 0.5$. The first column: $Ra = 10^4$ and the second: $Ra = 10^8$. The first row: $k_r = 1$, the second row: $k_r = 30$ and the third row: $k_r = 60$.

1 to 60 and the location of $|\Psi_{ext}|$ is almost the same. In this case, $|\Psi_{ext}|$ is considerably higher with respect to that in the cavity without fin, because a part of the cross section is blocked by a standing vortex above the fin and

to transport almost the same energy, the fluid convection hence $|\Psi_{ext}|$ is increased. The manifestation of these observations on the normalized Nusselt number has been as stated above discussing Fig. 5.

Following Fig. 4(c) with fin length, $W_P = 0.3$, Nu as a function of Ra is presented in Fig. 7(a) and (b) with $W_P = 0.5$ and 0.7 and keeping the other parameters the same as in Fig. 4. Fig. 7(a) shows that Nu is fin position dependent and similar to our observation in Fig. 4, it is minimum for $Y_P = 0.5$ at low Rayleigh numbers and the effect of fin position at $Ra > 10^7$ is not discernible. The decrease in Nu is 33% at $Ra = 10^4$ for $Y_P = 0.5$. It is from 5% to 3% for Ra from 10^7 to 10^9. Similar results are observed for $W_P = 0.7$ in Fig. 7(b) where again Nu is fin position dependent, it has the lowest value for $Y_P = 0.5$ at Ra between 10^4 and 10^7, and thereafter the fin position effect is not discernible. As expected, heat transfer suppression is further enhanced with longer fin: at $Ra = 10^4$, the decrease in Nu is 37%. These two cases were presented earlier as the last two columns in Fig. 4 for $Ra = 10^6$ and the mechanism of suppression was discussed. Similar figures are traced for the case of $W_P = 0.7$, $Y_P = 0.5$ in Fig. 7(b) for $Ra = 10^4$ and 10^8 and presented in Fig. 8. For $Ra = 10^4$, $|\Psi_{ext}| = 1.41$ at $(X = 0.66, Y = 0.75)$, which may be compared to $|\Psi_{ext}| = 5.8$ of the cavity without fin. We see that compared to the reference case, the heat transfer is suppressed considerably. Two symmetric cells are formed one below and the other above the fin. The strength of the cell above the fin is a little larger than that below due to higher local heat transfer in the upper part of the cavity. The isotherms on the right show quasi-conductive flow. At $Ra = 10^8$, the streamlines show similar pattern to that in Fig. 3 and $|\Psi_{ext}| = 68.95$ at $(X = 0.81, Y = 0.46)$ is quite enhanced compared to that for $Ra = 10^6$. In this case also, $|\Psi_{ext}|$ is considerably enhanced with respect to that of the cavity without fin, which is 56.98 (see Table 1). The reason is the same as discussed for Fig. 6. As expected, the isotherms on the right show a stratified flow at this high Rayleigh number. Indeed, we have seen in Figs. 4, 5 and 7 that for Rayleigh numbers above 10^7, the effects of geometrical and thermal parameters are not easily discernible. As mentioned earlier, the streamlines and isotherms for high Rayleigh numbers from 10^7 to 10^9 showed that the flow was no longer quasi-conduction dominated but represented rather a stratified pattern as in Fig. 8.

5. Conclusions

Heat transfer by natural convection in differentially heated square cavities with horizontal thin fin has been numerically studied. The cavity was formed by vertical isothermal walls and adiabatic horizontal walls. A thin fin was attached to the hot wall. Its dimensionless length, W_P was varied from 0.10 to 0.90 and its dimensionless position, Y_P from 0.10 to 0.90. The relative conductivity of the thin fin, k_r was varied from 1 to 60. Rayleigh number was from 10^4 to 10^9.

Based on the findings in this study, we conclude that normalized Nusselt number, Nu is an increasing function of Rayleigh, Ra, and a decreasing function of fin length, W_P and relative conductivity ratio, k_r. There is always an optimum fin position, Y_P, which is often at the center or near center of the cavity, which makes heat transfer by natural convection minimized. There are however few cases with relative conductivity, $k_r = 1$ in which heat transfer is enhanced by few percent when the fin length is short and positioned near the insulated horizontal boundaries.

Fin having finite conductivity attached on a hot wall of a differentially heated square cavity modifies the flow and temperature fields. In comparison with an identical square cavity without fin, temperature fields in a cavity with fin manifest a quasi-conduction dominated regime

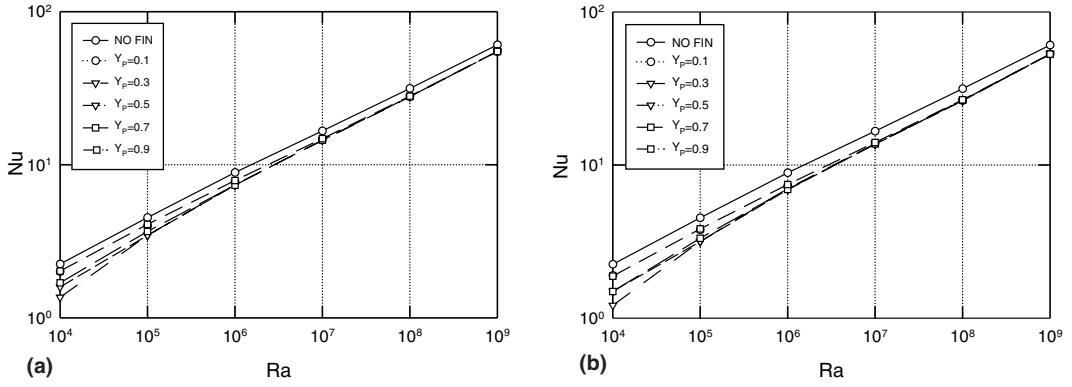

Fig. 7. Nusselt number as a function of Rayleigh number with $k_r = 30$, $W_P = 0.5$ and 0.7, and Y_P from 0.1 to 0.9 as parameters: (a) $k_r = 30$, $W_P = 0.5$ and $Y_P = 0.1$ to 0.9, (b) $k_r = 30$, $W_P = 0.7$ and $Y_P = 0.1$ to 0.9.

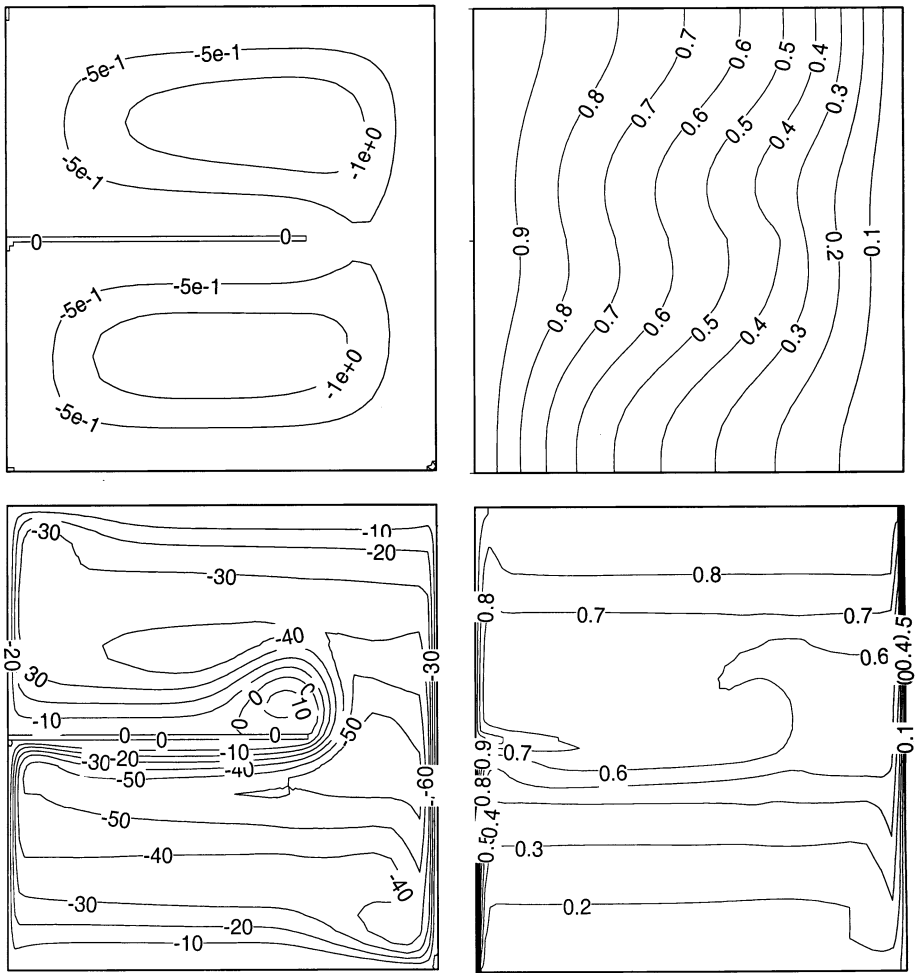

Fig. 8. Flow and temperature fields for $W_P = 0.7$ and $Y_P = 0.5$: The first row: $Ra = 10^4$ and the second row: $Ra = 10^8$. The flow field is on the left and the temperature field on the right.

at Rayleigh numbers from 10^4 to 10^7, thereafter they show a stratified flow. Conduction through the cavity is enhanced with fin and it becomes higher when the relative conductivity is higher, the fin length is longer and the fin's position is at or near the cavity center. On the other hand, natural convection is suppressed due to the presence of fin, which is intensified when the relative conductivity is higher, the fin is longer and the fin's position is at or near the cavity center. These counter-acting mechanisms determine the overall heat transfer through the cavity. Depending on the application, which may require maximizing or minimizing heat transfer, these two mechanisms can be used by choosing appropriate parameters such as Rayleigh number, relative conductivity and geometrical parameters. Although most of the applications could be those in which suppression of heat transfer by natural convection is desirable, few for heat transfer enhancement, such as electronic cooling, passive cooling in dwellings and radiators, can be designed by choosing appropriate geometrical and thermal fin parameters. We have seen that depending on the Rayleigh number, these parameters can be different, thus the design parameter selection should be done for each specific case.

Acknowledgement

Financial support by Natural Sciences and Engineering Research Council of Canada is acknowledged.

References

[1] R. Scosia, R.L. Frederick, Natural convection in slender cavities with multiple fins attached on an active wall, Num. Heat Transfer A 20 (1991) 127–158.

[2] G.N. Facas, Natural convection in a cavity with fins attached to both vertical walls, J. Thermophys. Heat Transfer 7 (1993) 555–560.
[3] E.K. Lakhal, M. Hasnaoui, E. Bilgen, P. Vasseur, Natural convection in inclined rectangular enclosures with perfectly conduction fins attached on the heated wall, Heat Mass Transfer 32 (1997) 365–373.
[4] S. Shakerin, M. Bohn, R.I. Loehrke, Natural convection in an enclosure with discrete roughness element on a vertical heated wall, Int., Heat Mass Transfer 31 (1988) 1423–1430.
[5] A. Nag, A. Sarkar, V.M.K. Sastri, Effect of thick horizontal partial partition attached to one of the active walls of a differentially heated square cavity, Num. Heat Transfer A 25 (1994) 611–625.
[6] E. Bilgen, Experimental study of massive wall systems with fins attached on the heated wall and with glazing, Heat Mass Transfer 38 (2001) 159–164.
[7] P.L. Oosthuizen, J.T. Paul, Free convection heat transfer in a cavity fitted with a horizontal plate on the cold wall, in: S.M. Shenkman et al. (Eds.), Advances in Enhanced Heat Transfer, vol. 43, ASME HTD, 1985, pp. 101–107.
[8] R.L. Frederick, Natural convection in an inclined square cavity with a partition attached to its cold wall, Int. J. Heat Mass Transfer 32 (1989) 87–94.
[9] R.L. Frederick, A. Valencia, Heat transfer in a square cavity with a conducting partition on its hot wall, Int. Commun. Heat Mass Transfer 16 (1989) 347–354.
[10] A. Nag, A. Sarkar, V.M.K. Sastri, Natural convection in a differentially heated square cavity with a horizontal partition plate on the hot wall, Comput. Meth Appl. Mech. Eng. 110 (1993) 143–156.
[11] X. Shi, J.M. Khodadadi, Laminar convection heat transfer in a differentially heated square cavity due to a thin fin on the hot wall, J. Heat Transfer 125 (2003) 624–634.
[12] S.V. Patankar, Numerical Heat Transfer and Fluid Flow, Hemisphere Publishing Corp., New York, 1980.
[13] R. Ben Yedder, E. Bilgen, Laminar natural convection in inclined enclosures bounded by a solid wall, Heat Mass Transfer 32 (1997) 455–462.
[14] G. De Vahl Davis, I.P. Jones, Natural convection in square cavity: a comparison exercise, Int. J. Num. Meth. Fluid 3 (1983) 227–248.